HHS Public Access

Author manuscript

Auton Neurosci. Author manuscript; available in PMC 2019 March 01.

Published in final edited form as:

Auton Neurosci. 2018 March ; 210: 44–54. doi:10.1016/j.autneu.2017.12.005.

Variable Expression of GFP in Different Populations of Peripheral Cholinergic Neurons of ChAT^{BAC}-eGFP Transgenic Mice

T. Christopher Brown[a], **Cherie E. Bond**[c], and **Donald B. Hoover**[a,b]

[a]Department of Biomedical Sciences, Quillen College of Medicine, East Tennessee State University, Johnson City, TN 37614, USA

[b]Center of Excellence in Inflammation, Infectious Disease and Immunity, East Tennessee State University, Johnson City, TN 37614, USA

[c]School of Natural Sciences and Mathematics, Ferrum College, Ferrum, VA 24088, USA

Abstract

Immunohistochemistry is used widely to identify cholinergic neurons, but this approach has some limitations. To address these problems, investigators developed transgenic mice that express enhanced green fluorescent protein (GFP) directed by the promoter for choline acetyltransferase (ChAT), the acetylcholine synthetic enzyme. Although, it was reported that these mice express GFP in all cholinergic neurons and non-neuronal cholinergic cells, we could not detect GFP in cardiac cholinergic nerves in preliminary experiments. Our goals for this study were to confirm our initial observation and perform a qualitative screen of other representative autonomic structures for the presences of GFP in cholinergic innervation of effector tissues. We evaluated GFP fluorescence of intact, unfixed tissues and the cellular localization of GFP and vesicular acetylcholine transporter (VAChT), a specific cholinergic marker, in tissue sections and intestinal whole mounts. Our experiments identified two major tissues where cholinergic neurons and/or nerve fibers lacked GFP: 1) most cholinergic neurons of the intrinsic cardiac ganglia and all cholinergic nerve fibers in the heart and 2) most cholinergic nerve fibers innervating airway smooth muscle. Most cholinergic neurons in airway ganglia stained for GFP. Cholinergic systems in the bladder and intestines were fully delineated by GFP staining. GFP labeling of input to ganglia with long preganglionic projections (vagal) was sparse or weak, while that to ganglia with short preganglionic projections (spinal) was strong. Total absence of GFP might be due to splicing out of the GFP gene. Lack of GFP in nerve projections from GFP-positive cell bodies might reflect a transport deficiency.

Corresponding author: Dr. Donald B. Hoover, Department of Biomedical Sciences, Quillen College of Medicine and Center of Excellence in Inflammation, Infectious Disease and Immunity, East Tennessee State University, Johnson City, TN 37614, USA, Phone +1 423 439 6322, Fax +1 423 439 8044, hoover@etsu.edu.

Keywords

ChAT^{BAC}-eGFP transgenic mice; cholinergic markers; enteric nervous system; intrinsic cardiac neurons; parasympathetic nervous system; immunohistochemistry

1. Introduction

Localization of cholinergic neurons in the central and peripheral nervous systems was accomplished initially using histochemistry for acetylcholinesterase, but this approach yielded some false positive results (Koelle, 1963; Hoover et al., 2004). Increased knowledge about the neurochemistry of cholinergic neurons and elucidation of the amino acid sequence of proteins that are required for the synthesis and storage of acetylcholine (ACh) in cholinergic neurons has led to the production of specific antibodies, which have been instrumental in the localization of cholinergic neurons and their processes in the central nervous system and periphery. Specific proteins targeted for immunohistochemistry are the high affinity choline transporter (CHT1) required for uptake of choline at cholinergic nerve endings (Misawa et al., 2001; Kus et al., 2003; Hoover et al., 2004), the ACh synthetic enzyme choline acetyltransferase (ChAT) (Kimura et al., 1980; Woolf, 1991), and the vesicular ACh transporter (VAChT) needed for storage of ACh in secretory vesicles (Weihe et al., 1996; Arvidsson et al., 1997; Schafer et al., 1998; Schäfer et al., 1998). Antibodies to cholinergic proteins can vary in their sensitivity for detection of the specific antigen and in the amount of background staining. The utility of polyclonal antibodies can also vary between lots. Variations in the structure of ChAT have been noted and probably contribute to the limited efficacy of ChAT antibodies for labeling all cholinergic perikarya and processes in the autonomic nervous system (Bellier and Kimura, 2011).

To overcome problems in detection of ChAT in peripheral neurons and to enable *in vivo* identification of central and peripheral cholinergic neurons and nerve fibers, some investigators have used a bacterial artificial chromosome strategy to insert an enhanced green fluorescent protein (GFP) gene into the ChAT locus (Tallini et al., 2006). It was reported that this approach results in the expression of GFP in central and peripheral cholinergic neurons and in non-neuronal cholinergic cells (Tallini et al., 2006).

ChAT^{BAC}-eGFP mice have been used extensively in recent years to identify and facilitate the study of cholinergic immune cells, specifically T and B cells (Rosas-Ballina et al., 2011; Reardon et al., 2013). We purchased these transgenic mice primarily for this purpose and have confirmed their value for detecting abundant cholinergic leukocytes in the spleen and mesenteric lymph node (Hoover, 2017). Additionally, we have a long-term interest in cardiac cholinergic innervation and regulatory mechanisms, so we decided to evaluate the utility of ChAT^{BAC}-eGFP mice for localizing cardiac parasympathetic neurons and the distribution of their projections within the myocardium. The original report on the ChAT^{BAC}-eGFP strain suggested a broad utility of these mice for study of the parasympathetic innervation, but no convincing data were reported for the heart and intrinsic cardiac ganglia. Surprisingly, our preliminary experiments did not identify GFP+ nerve fibers in the myocardium of ChAT^{BAC}-eGFP mice. Accordingly, our goals for this study were to confirm our initial

observation for heart and to perform a qualitative screen of other representative autonomic structures for the presences of GFP in cholinergic innervation of effector tissues. The results demonstrate that GFP is not expressed uniformly throughout the autonomic nervous system. Deficits are prominent in the heart, airway smooth muscle, and terminals of long preganglionic cholinergic nerve fibers.

2. Materials and methods

2.1. Animals

Male and female B6.Cg-Tg(RP23-268L19 EGFP)2Mik/J mice, also known as ChAT^{BAC}-eGFP mice, were obtained from The Jackson Laboratory (Bar Harbor, ME) and bred in house. Adult, male offspring were used for this study (n=12). Major observations were replicated using tissue from three separate mice. Animal protocols were approved by the East Tennessee State University Animal Care and Use Committee and conformed to guidelines of the National Institutes of Health as published in the *Guide for the Care and Use of Laboratory Animals* (Eighth Edition, National Academy of Sciences, 2011).

2.2. Tissue collection and processing

Mice were euthanized with isoflurane for tissue collection. For experiments using frozen sections, the mice were perfused transcardially (10 ml/min) with 40 ml of 0.1 M phosphate buffered saline (PBS, pH 7.3) containing heparin (1U/ml) followed by 40 ml of 4% paraformaldehyde (PFA) in PBS. Tissues were collected and stored in fixative overnight at 4°C, rinsed in PBS, and cryoprotected by storage in 20% sucrose in PBS at 4 °C for about 3 days. Tissues were then stored at −80° C until sectioning. Frozen 30 μm sections were cut at −14° C using a Leica CM 3050S cryostat and collected on charged slides. Slide-mounted sections were stored at −80° C in slide boxes wrapped in aluminum foil.

Separate animals were used to prepare whole mounts from the intestines. The gastrointestinal tract (GI) was removed intact from the level of the fundus of the stomach to the rectum and placed in cold 0.1M PBS. The duodenum was cannulated with a gavage needle and secured using surgical silk. The lumen was flushed using ice cold PBS followed by 4% PFA in PBS, the rectal end tied, and the GI tract was inflated using cold fixative. Specific regions of the GI tract were tied off and removed while inflated. These segments of GI tract were post-fixed overnight at 4 °C, washed in PBS, opened at both ends, cut longitudinally, and pinned to a Petri dish. After washing with PBS, villi and mucosal layers were removed from some segments by gentle scraping with a cotton swab. Resulting whole mounts were stained free floating.

GFP fluorescence of unfixed tissue was evaluated in some cases by confocal microscopy or by use of an Olympus SZ stereomicroscope fitted with a Nightsea fluorescence adaptor that included a royal blue light and filter set (Electron Microscopy Sciences, Hatfield, PA). Stereomicroscopic images were collected with a MagnaFire SP digital camera. For confocal microscopy, tissue was wet with a small amount of Citifluor AF1 mountant media and placed on a 35-mm glass bottom culture dish (MatTek, Ashland, MA).

2.3. Immunohistochemistry

Frozen, cryostat sections were slowly brought to room temperature for staining by routine immunofluorescence methods as described previously (Hoover et al., 2004; Mabe et al., 2006; Downs et al., 2014). Slides were washed in 0.1 M PBS followed by PBS containing 0.5% bovine serum albumin (BSA) + 0.4% Triton X-100 in PBS and then blocked for 2 h in PBS containing 5% normal donkey serum + 1% BSA + 0.4% Triton X-100. Sections were then washed in PBS and incubated overnight in the same blocking solution plus primary antibodies: rabbit anti-VAChT (Synaptic Systems, Gottingen, Germany, catalog # 139 103) at a dilution of 1:500 and chicken anti-GFP (Abcam, Cambridge, MA, catalog # ab 290) at 1:1000. After washing and blocking again, tissues were incubated for 2 h in the following secondary antibodies at 1:200 dilution: Alexa Fluor 488-conjugated donkey anti-chicken (Jackson ImmunoResearch, West Grove, PA, USA) and Alexa Fluor 594-conjugated donkey anti-rabbit (Invitrogen/Thermo Fisher Scientific Rockford, IL or Jackson ImmunoResearch, West Grove, PA, USA). For some experiments, fluorphores conjugated to the secondary antibodies were switched, using Alexa Fluor 488 to detect VAChT and Alexa Fluor 594 to detect GFP. After washing the slides with PBS, cover glasses were attached using Citifluor mounting medium (Ted Pella, Redding, CA, USA) and sealed with clear nail polish.

Whole mounts of intestine were stained free floating in 12-well plates as described for slide-mounted sections except for incubations in primary and secondary antibodies and the use of more extensive washing after these steps. Whole mounts were incubated in primary and secondary antibodies for 48 h at 4° C with gentle oscillation on an orbital shaker. After the final washing in PBS, whole mounts were transferred to slides, spread out, and excess PBS was removed prior to applying Citifluor and a cover glass. A weight was placed on top of the cover glass before sealing with nail polish and remained overnight while the polish hardened.

2.4. Microscopy and collection of images

Slide-mounted sections were viewed using an Olympus BX4 fluorescence microscope and a Leica TCS SP8 Confocal Microscope. Digital images were obtained from the fluorescence microscope using an attached Olympus Q-Color 3 digital camera and Q-Cap Pro 7 software. Whole mounts were viewed and digital images collected using a Leica TCS SP8 Confocal Microscope. Confocal images were collected by single channel scans with a 488 laser for GFP fluorescence (unfixed tissue) and by sequential scans using 488 and 552 laser lines for double labeled preparations. Maximum projection images were created from stacks of optical sections collected across the full thickness of tissues sections. Details for confocal images of fresh trachea and whole mounts of intestine are provided in figure legends.

3. Results

3.1 Cardiac cholinergic nerves and most perikarya of the intrinsic cardiac ganglia lack GFP in ChAT^{BAC}-eGFP mice

Short-axis sections of the heart, from the anterior pole through the bundle of His, were evaluated by double labeling for VAChT and GFP. Previous studies have established that cholinergic innervation is abundant throughout this region of the heart, being especially

dense in nodal regions and the atrioventricular (AV) conducting system (Hoover et al., 2004; Mabe et al., 2006). Our staining for VAChT replicates previous findings, as shown in figures 1 and 2 for the right atrium and ventricle, sinoatrial node (SAN), interatrial septum, AV node (AVN), left atrium and ventricle, bundle of His, and interventricular septum. In all cases, VAChT-positive cholinergic nerve fibers in the heart lacked staining for GFP in the same sections. This was true regardless of the fluorophore used to detect GFP (Alexa Fluor 488: Fig. 1E and H, Fig. 2A; Alexa Fluor 594: Fig. 1A, Fig. 1E and H). Additionally, prominent staining for GFP was evident in airway epithelial cells of bronchi and trachea, which were attached to the dorsal surface of the atrium (Fig. 7). These findings argue that lack of GFP staining in cardiac cholinergic nerve fibers was due to absence of the marker.

Neurons of the intrinsic cardiac ganglia, which provide cholinergic innervation of the heart, showed light-to-moderate staining for VAChT and were surrounded by prominent, VAChT-positive varicosities (Fig. 3A and C). These cholinergic varicosities are vagal efferent innervation of the ganglia. In marked contrast, intrinsic cardiac neurons rarely stained for GFP (Fig. 3B and C) and GFP-positive varicosities were sparse or absence in the intrinsic cardiac ganglia (Fig. 3B and C). This contrasts with sympathetic ganglia (Fig. 5) and the major pelvic ganglia (Fig. 3G–H) where prominent staining for GFP was present in preganglionic cholinergic innervation. GFP fluorescence of unfixed tissues allowed visualization of the sympathetic chain ganglia, the celiac-superior mesenteric ganglion, and major pelvic ganglia (Figs. 4A–C) by fluorescence stereomicroscopy, but the ganglionated nerve plexus on the dorsal atrium of the mouse heart (Mabe et al., 2006; Rysevaite et al., 2011a; Rysevaite et al., 2011b) could not be detected by this method (Fig. 4E and F). In marked contrast, the ganglionated nerve plexus of the enteric nervous system showed bright fluorescence when viewed from the serosal surface (Fig. 4D).

3.2. GFP is absent in most cholinergic nerve fibers supplying airway smooth muscle but occurs in a subpopulation of airway epithelial cells

GFP fluorescence of unfixed trachea was evaluated by viewing the surface with underlying smooth muscle by fluorescence stereomicroscopy (Fig. 6A). No GFP signal was detected in this region, even by using a long exposure. Likewise, imaging of unfixed tracheal rings by confocal microscopy failed to detect GFP in cholinergic innervation of tracheal smooth muscle, but this approach did reveal strong GFP signal in tracheal epithelial cells (Fig. 6B).

Bronchi and trachea were present in some sections through the heart, and additional sections through the cervical trachea were collected and evaluated by double labeling for VAChT and GFP. VAChT-positive cholinergic nerves stained intensely and were abundant in bronchial (Fig. 3D and F; Fig. 7G and I) and tracheal smooth muscle (Fig. 7A and C). Most of these nerves lacked staining for GFP (Fig. 3E and F; Fig. 7B, C, H, and I), and those that did stain for GFP required confocal microscopy for definitive demonstration (Fig. 7G–I). When present in airway smooth muscle, GFP staining was less intense than that for VAChT and occurred in fewer fibers located primarily in the outer smooth muscle layers (Fig. 7G–I). A few VAChT-positive nerves also occurred in the subepithelial region of the airways, and these fibers occasionally stained for GFP (Fig. 7D–F). In marked contrast, a subpopulation of airway epithelial cells stained strongly for GFP (Fig. 7). Most of these cells lacked

VAChT when viewed by standard fluorescence microscopy, but VAChT could be detected in several GFP-positive epithelial cells by confocal microscopy (Fig. 7D–F).

Airway ganglia were not abundant in our sections, but cholinergic neurons of these ganglia often expressed GFP (Fig. 3D–F; Fig. 7A–C). Neurons in these ganglia were surrounded by VAChT-positive varicosities, which often lacked GFP.

3.3. GFP is expressed in cholinergic neurons of the major pelvic ganglia and in cholinergic nerve fibers that innervated the bladder

The major pelvic ganglia contain cholinergic and noradrenergic neurons (Elfvin et al., 1997; Wanigasekara et al., 2003; Pidsudko, 2014) and provide cholinergic innervation of the bladder (Pidsudko, 2014). As noted previously, fluorescence from GFP was strong enough to visualize these ganglia and nerve bundles projecting to the bladder using a stereomicroscope (Fig. 4C). Long-axis sections through pelvic ganglia and bladder were used to evaluate the cellular and regional localization of eGFP to cholinergic neurons and nerve fibers by double labeling for VAChT and GFP. Extensive overlap of staining for GFP and VAChT was observed for this system. Many cell bodies in the pelvic ganglia at the base of the bladder, stained intensely for GFP and lightly or not at all for VAChT, but presumed noradrenergic neurons lacked both markers (Fig. 3 G–I). Most neurons of the pelvic ganglia were surrounded by nerve processes that stained for GFP and VAChT (Fig. 3 G–I). Smooth muscle layers of the bladder wall showed densely packed nerve fibers staining for VAChT and substantial colocalization of GFP with VAChT (Fig. 8). VAChT and GFP were also colocalized in a smaller number of cholinergic nerve fibers in the bladder mucosa (Fig. 8A–F).

3.4. GFP is expressed by preganglionic cholinergic neurons, lower motor neurons, and cholinergic neurons of the enteric nervous system

Double staining of frozen sections from the medulla oblongata and lumbar level of the spinal cord confirmed the localization of GFP to preganglionic parasympathetic neurons in the dorsal motor nucleus of the vagus (Fig. 9A–C) and nucleus ambiguus (Fig. 9D–F), preganglionic sympathetic neurons in the intermediolateral cell column (Fig. 9G–I) and to lower motor neurons in the hypoglossal nucleus (Fig. 9A–C) and ventral horn (Fig. 9G–I). VAChT and GFP were also colocalized in preganglionic, cholinergic nerve projections to sympathetic ganglia, but neither marker was detected in postganglionic sympathetic neurons (Fig. 5).

As noted earlier, stereomicroscopic evaluation of unfixed duodenum demonstrated strong, fluorescence of GFP in ganglia and nerve bundles of the enteric nervous system (Fig. 4D). Localization of GFP to cholinergic neurons and nerve fibers was confirmed by confocal analysis of fixed whole mount preparations of duodenum, jejunum, and ileum, as described in the methods. Many cholinergic neurons of the enteric nervous system showed intense fluorescence for GFP but were not stained for VAChT (Fig. 10A–F). VAChT and GFP were both localized to the extensive nerve plexus in the enteric nervous system (Fig. 10A–F) and to nerve fibers within the intestinal villi (Fig. 10G–I). Numerous varicosities around enteric neurons stained intensely for VAChT (Fig. 10D and F), but GFP-positive varicosities were

less abundant and did not stain intensely (Fig. 10D–F). Scattered epithelial cells throughout the villi stained intensely for GFP but lacked VAChT (Fig. 10G–I).

4. Discussion

The ChAT^{BAC}-eGFP transgenic mouse model was developed to facilitate the identification and study of cholinergic neurons and nerve fibers in the central and peripheral nervous systems (Tallini et al., 2006), and it has been used widely for this purpose based on over 70 citations of the work identified through Web of Science. We assumed that all cholinergic neurons would express GFP in their soma and throughout their processes. However, our preliminary experiments failed to identify GFP in cardiac parasympathetic neurons. Based on this observation, we performed a qualitative screen of representative autonomic neurons and their peripheral targets in ChAT^{BAC}-eGFP mice to determine the expression of GFP in the perikarya and terminal fields of known cholinergic neurons. This study identified two major sites where cholinergic neurons lacked GFP: 1) most cholinergic neurons of the intrinsic cardiac ganglia and all cholinergic nerve fibers in the heart and 2) most cholinergic nerve fibers innervating airway smooth muscle. We have not identified any previous studies of these sites in ChAT^{BAC}-eGFP mice of other transgenic mice with tagged cholinergic neurons. Additionally, we found that staining for GFP was absent, sparse, and/or low intensity in vagal efferent projections to the intrinsic cardiac, airway, and enteric ganglia but abundant and intense in shorter preganglionic projections to sympathetic and major pelvic ganglia. Expression of GFP was detected at all other sites evaluated. A summary of all our findings is presented in Table 1.

The ChAT^{BAC}-eGFP transgenic mice used in this study were created by using a bacterial artificial chromosome (BAC) construct that contains the entire cholinergic gene locus, including upstream promoter regions (Tallini et al., 2006). This BAC was constructed with the GFP gene cassette inserted at the start site for translation of ChAT and was linked to a poly-A signal that terminates translation of the mRNA into protein. Thus, when GFP is expressed under the control of the ChAT promoter, it precludes expression of ChAT protein. Since BACs insert somewhat randomly into the genome, they are not necessarily inserted in or near the gene locus of interest. In the ChAT^{BAC}-GFP transgenic mice, three copies of the GFP cassette were inserted into their genomes (Nagy and Aubert, 2012). Therefore, in cells expressing the transcription factors for the cholinergic locus: (1) one copy of the ChAT gene is expressed just as in wild-type mice; (2) GFP mRNA and protein expression is 2–3X higher than ChAT expression; and (3) because the VAChT gene is embedded in the cholinergic locus, VAChT mRNA and protein expression are 2X and 1.5–1.7X higher, respectively, if transcription factors that bind to its promoter are present (Nagy and Aubert, 2012; Nagy and Aubert, 2013). Accordingly, it is valid to use GFP fluorescence/staining as an indicator for the presence of ChAT, regardless of the isoform(s) expressed. Furthermore, VAChT abundance should be elevated in cells where it is expressed since the ChAT^{BAC}-eGFP transgenic mice have four copies of the gene locus.

ChAT, CHT1, and VAChT are synthesized in the neuronal soma and transported to neuronal varicosities where synthesis, storage, and release of ACh occurs (Prado et al., 2002; Westfall TC, 2006). Thus, all three cholinergic markers are expected to concentrate in nerve

processes that innervate target cells in the CNS and periphery. The relative abundance of cholinergic markers in neuronal somata would depend on rates of synthesis and subsequent transport to distal processes. The importance of axonal transport in affecting soma levels of CHT1 in cardiac parasympathetic neurons was demonstrated in experiments with whole mount preparations of atrial ganglionated plexus from the guinea pig (Hoover et al., 2004). Immunolabeling for CHT1 is normally low or absent in these neurons *in situ* and after three days in culture. However, treatment of whole mounts with colchicine to block axoplasmic transport caused a robust increase in CHT1 immunoreactivity of ganglionic neurons after three days. Our observations on the localization of VAChT to known cholinergic neurons and nerve fibers are consistent with these cellular considerations and findings from previous immunohistochemical studies (Gilmor et al., 1996; Li et al., 1998; Schafer et al., 1998; Schütz et al., 2015).

The most striking discrepancy between GFP and VAChT in our study occurred in the heart and airway smooth muscle. VAChT was localized to cholinergic neurons in regional ganglia and to the numerous cholinergic nerves that innervate the myocardium and airway smooth muscle, but cholinergic nerves in the heart and most cholinergic nerves in airway smooth muscle lacked GFP. The absence of GFP in most intrinsic cardiac neurons suggests that the GFP gene is not transcribed in these neurons, and this would account for the total absence of GFP in cholinergic innervation of the heart. It is conceivable that a splice variant of ChAT exists in mice that skips the exon containing GFP in the intrinsic cardiac neurons. In fact, previous work demonstrated that alternative splicing of ChAT mRNA can occur, yielding seven different variants of cChAT (Misawa et al., 1992) that produce proteins of identical molecular weight of approximately 67 kDa. While the number of airway ganglia present in our samples was small, most of the neurons in these ganglia did express GFP at a moderate level of intensity, so a different mechanism must account for the lack of GFP in most VAChT-positive nerves supplying bronchial and tracheal smooth muscle. Although the axons of these neurons would be relatively short, it is possible that a defect in GFP axonal transport might exist. Inefficient axonal transport of GFP might explain the light staining of nerve fibers for GFP in outer smooth muscle layers of the airways, which are presumably closer to the ganglia, and the absence of detectable GFP in most VAChT-positive nerve fibers.

We observed that colocalization of GFP with VAChT in preganglionic innervation appeared to vary between autonomic ganglia. Sympathetic ganglia and the major pelvic ganglia showed extensive colocalization of both markers in perineuronal nerve fibers and varicosities, while neurons in cardiac, airway, and enteric ganglia where surrounded primarily by VAChT-positive varicosities. We believe that this difference could be due to inefficient transport of GFP. Preganglionic axons to the sympathetic and pelvic ganglion emanate from cell bodies at corresponding levels of the spinal cord and are relatively short. In contrast, preganglionic input to the cardiac, airway, and enteric ganglia comprises longer axons from vagal efferent neurons located in the medulla oblongata. These observations and our data for airway cholinergic neurons suggest that axonal transport of GFP likely differs from that of native cholinergic proteins (i.e., VAChT and CHT1), and therefore, it can provide less robust labeling of terminal innervation at some sites.

While evaluating the expression of GFP by peripheral cholinergic neurons was the primary goal of this study, we also observed prominent staining for GFP in scattered epithelial cells of the airways and in the small intestine of the same preparations that were used to evaluate the neuronal localization of GFP and VAChT. This observation confirms previous findings from other studies that used the same ChAT^{BAC}-eGFP transgenic mice to examine cholinergic epithelial cells (Kummer and Krasteva-Christ, 2014; Krasteva-Christ et al., 2015; Schütz et al., 2015). Analysis of double-labeled tissues by confocal microscopy revealed that some GFP+ epithelial cells in the airways exhibited low to moderate intensity of staining for VAChT, but epithelial cells in the small intestine lacked VAChT. The lack of VAChT in epithelial cells of the small intestine in our study concurs with results from a previous extensive evaluation of cholinergic epithelial cells throughout the mouse gastrointestinal tract (Schütz et al., 2015). These investigators found GFP+/ChAT+ epithelial cells at all levels of the tract except the anal canal, and co-expression of VAChT was restricted to cholinergic epithelial cells in the proximal portion of the large intestine. Likewise, our observation of VAChT in cholinergic epithelial cells of the airways concurs with published data for tracheal epithelial cells (Krasteva et al., 2011). The lack of VAChT in non-neuronal cholinergic cells, such as intestinal epithelial cells, indicates that release of ACh from these cells does not occur by a vesicular mechanism involving exocytosis. Instead, polyspecific organic cation transporters have been identified that are capable of mediating constitutive release of ACh (Kummer and Krasteva-Christ, 2014).

In summary, this study has confirmed the utility of ChAT^{BAC}-eGFP transgenic mice for identification of many cholinergic neurons and non-neuronal cells in the periphery but also found a few limitations of this model. First and foremost, GFP is not detectable in cardiac parasympathetic neurons and nerve fibers. This finding could reflect unique transcription processes at the cholinergic gene locus in these neurons. Consequently, terminal processes of these neurons lacked GFP. Additionally, we observed that GFP was not a suitable marker for cholinergic nerve fibers that innervate bronchial and tracheal smooth muscle. For most applications, the ChAT^{BAC}-eGFP transgenic mice remain a valuable tool for localization of cholinergic neurons and non-neuronal cells *in vivo* or *in vitro* by using fluorescence of GFP in unfixed tissue or immunohistochemical detection in fixed tissues.

Acknowledgments

The authors are grateful to Rolf Fritz for confocal microscopy. This work was supported by the National Institute of Health (R15GM107949, 2014 to D.B.H. and C06RR0306551).

Abbreviations

ANS	autonomic nervous system
BSA	bovine serum albumin
ChAT	choline acetyltransferase
pChAT	peripheral choline acetyltransferase
GFP	enhanced green fluorescent protein

NDS	normal donkey serum
PBS	phosphate-buffered saline
VAChT	vesicular acetylcholine transporter

References

Arvidsson U, Riedl M, Elde R, Meister B. Vesicular acetylcholine transporter (VAChT) protein: a novel and unique marker for cholinergic neurons in the central and peripheral nervous systems. J Comp Neurol. 1997; 378:454–467. [PubMed: 9034903]

Bellier JP, Kimura H. Peripheral type of choline acetyltransferase: biological and evolutionary implications for novel mechanisms in cholinergic system. J Chem Neuroanat. 2011; 42:225–235. [PubMed: 21382474]

Downs AM, Bond CE, Hoover DB. Localization of alpha7 nicotinic acetylcholine receptor mRNA and protein within the cholinergic anti-inflammatory pathway. Neuroscience. 2014; 266:178–185. [PubMed: 24561218]

Elfvin LG, Holmberg K, Emson P, Schemann M, Hökfelt T. Nitric oxide synthase, choline acetyltransferase, catecholamine enzymes and neuropeptides and their colocalization in the anterior pelvic ganglion, the inferior mesenteric ganglion and the hypogastric nerve of the male guinea pig. J Chem Neuroanat. 1997; 14:33–49. [PubMed: 9498165]

Gilmor ML, Nash NR, Roghani A, Edwards RH, Yi H, Hersch SM, Levey AI. Expression of the putative vesicular acetylcholine transporter in rat brain and localization in cholinergic synaptic vesicles. J Neurosci. 1996; 16:2179–2190. [PubMed: 8601799]

Hoover DB. Cholinergic modulation of the immune system presents new approaches for treating inflammation. Pharmacol Ther. 2017; 179:1–16. [PubMed: 28529069]

Hoover DB, Ganote CE, Ferguson SM, Blakely RD, Parsons RL. Localization of cholinergic innervation in guinea pig heart by immunohistochemistry for high-affinity choline transporters. Cardiovasc Res. 2004; 62:112–121. [PubMed: 15023558]

Kimura H, McGeer PL, Peng F, McGeer EG. Choline acetyltransferase-containing neurons in rodent brain demonstrated by immunohistochemistry. Science. 1980; 208:1057–1059. [PubMed: 6990490]

Koelle GB. Cytological distributions and physiological functions of cholinesterases. Handb Exp Pharmacol. 1963; 15:187–298.

Krasteva-Christ G, Soultanova A, Schütz B, Papadakis T, Weiss C, Deckmann K, Chubanov V, Gudermann T, Voigt A, Meyerhof W, Boehm U, Weihe E, Kummer W. Identification of cholinergic chemosensory cells in mouse tracheal and laryngeal glandular ducts. Int Immunopharmacol. 2015; 29:158–165. [PubMed: 26033492]

Krasteva G, Canning BJ, Hartmann P, Veres TZ, Papadakis T, Mühlfeld C, Schliecker K, Tallini YN, Braun A, Hackstein H, Baal N, Weihe E, Schütz B, Kotlikoff M, Ibanez-Tallon I, Kummer W. Cholinergic chemosensory cells in the trachea regulate breathing. Proc Natl Acad Sci U S A. 2011; 108:9478–9483. [PubMed: 21606356]

Kummer W, Krasteva-Christ G. Non-neuronal cholinergic airway epithelium biology. Curr Opin Pharmacol. 2014; 16:43–49. [PubMed: 24681350]

Kus L, Borys E, Ping Chu Y, Ferguson SM, Blakely RD, Emborg ME, Kordower JH, Levey AI, Mufson EJ. Distribution of high affinity choline transporter immunoreactivity in the primate central nervous system. J Comp Neurol. 2003; 463:341–357. [PubMed: 12820166]

Li JY, Dahlström AM, Hersh LB, Dahlström A. Fast axonal transport of the vesicular acetylcholine transporter (VAChT) in cholinergic neurons in the rat sciatic nerve. Neurochem Int. 1998; 32:457–467. [PubMed: 9676745]

Mabe AM, Hoard JL, Duffourc MM, Hoover DB. Localization of cholinergic innervation and neurturin receptors in adult mouse heart and expression of the neurturin gene. Cell Tissue Res. 2006; 326:57–67. [PubMed: 16708241]

Misawa H, Ishii K, Deguchi T. Gene expression of mouse choline acetyltransferase. Alternative splicing and identification of a highly active promoter region. J Biol Chem. 1992; 267:20392–20399. [PubMed: 1400357]

Misawa H, Nakata K, Matsuura J, Nagao M, Okuda T, Haga T. Distribution of the high-affinity choline transporter in the central nervous system of the rat. Neuroscience. 2001; 105:87–98. [PubMed: 11483303]

Nagy PM, Aubert I. Overexpression of the vesicular acetylcholine transporter increased acetylcholine release in the hippocampus. Neuroscience. 2012; 218:1–11. [PubMed: 22641085]

Nagy PM, Aubert I. B6eGFPChAT mice overexpressing the vesicular acetylcholine transporter exhibit spontaneous hypoactivity and enhanced exploration in novel environments. Brain Behav. 2013; 3:367–383. [PubMed: 24381809]

Pidsudko Z. Immunohistochemical characteristics and distribution of neurons in the paravertebral, prevertebral and pelvic ganglia supplying the urinary bladder in the male pig. J Mol Neurosci. 2014; 52:56–70. [PubMed: 24122239]

Prado MA, Reis RA, Prado VF, de Mello MC, Gomez MV, de Mello FG. Regulation of acetylcholine synthesis and storage. Neurochem Int. 2002; 41:291–299. [PubMed: 12176069]

Reardon C, Duncan GS, Brüstle A, Brenner D, Tusche MW, Olofsson PS, Olofsson P, Rosas-Ballina M, Tracey KJ, Mak TW. Lymphocyte-derived ACh regulates local innate but not adaptive immunity. Proc Natl Acad Sci U S A. 2013; 110:1410–1415. [PubMed: 23297238]

Rosas-Ballina M, Olofsson PS, Ochani M, Valdés-Ferrer SI, Levine YA, Reardon C, Tusche MW, Pavlov VA, Andersson U, Chavan S, Mak TW, Tracey KJ. Acetylcholine-synthesizing T cells relay neural signals in a vagus nerve circuit. Science. 2011; 334:98–101. [PubMed: 21921156]

Rysevaite K, Saburkina I, Pauziene N, Noujaim SF, Jalife J, Pauza DH. Morphologic pattern of the intrinsic ganglionated nerve plexus in mouse heart. Heart Rhythm. 2011a; 8:448–454. [PubMed: 21075216]

Rysevaite K, Saburkina I, Pauziene N, Vaitkevicius R, Noujaim SF, Jalife J, Pauza DH. Immunohistochemical characterization of the intrinsic cardiac neural plexus in whole-mount mouse heart preparations. Heart Rhythm. 2011b; 8:731–738. [PubMed: 21232628]

Schäfer MK, Eiden LE, Weihe E. Cholinergic neurons and terminal fields revealed by immunohistochemistry for the vesicular acetylcholine transporter. I. Central nervous system. Neuroscience. 1998; 84:331–359. [PubMed: 9539209]

Schafer MK, Eiden LE, Weihe E. Cholinergic neurons and terminal fields revealed by immunohistochemistry for the vesicular acetylcholine transporter. II. The peripheral nervous system. Neuroscience. 1998; 84:361–376. [PubMed: 9539210]

Schütz B, Jurastow I, Bader S, Ringer C, von Engelhardt J, Chubanov V, Gudermann T, Diener M, Kummer W, Krasteva-Christ G, Weihe E. Chemical coding and chemosensory properties of cholinergic brush cells in the mouse gastrointestinal and biliary tract. Front Physiol. 2015; 6:87. [PubMed: 25852573]

Tallini YN, Shui B, Greene KS, Deng KY, Doran R, Fisher PJ, Zipfel W, Kotlikoff MI. BAC transgenic mice express enhanced green fluorescent protein in central and peripheral cholinergic neurons. Physiol Genomics. 2006; 27:391–397. [PubMed: 16940431]

Wanigasekara Y, Kepper ME, Keast JR. Immunohistochemical characterisation of pelvic autonomic ganglia in male mice. Cell Tissue Res. 2003; 311:175–185. [PubMed: 12596037]

Weihe E, Tao-Cheng JH, Schäfer MK, Erickson JD, Eiden LE. Visualization of the vesicular acetylcholine transporter in cholinergic nerve terminals and its targeting to a specific population of small synaptic vesicles. Proc Natl Acad Sci U S A. 1996; 93:3547–3552. [PubMed: 8622973]

Westfall, TC., Westfall, DP. Neurotransmission: The autonomic and somatic motor nervous systems. In: Brunton, LL., editor. Goodman and Gilman's the pharmacological basis of therapeutics. 11th. McGraw-Hill; New York: 2006. p. 137-181.

Woolf NJ. Cholinergic systems in mammalian brain and spinal cord. Prog Neurobiol. 1991; 37:475–524. [PubMed: 1763188]

Highlights

- ChAT^{BAC}-eGFP mice are used to identify cholinergic neurons and non-neuronal cells but some cholinergic neurons lack GFP.
- Most cholinergic neurons of the cardiac ganglia within the chest and all of their projections lack GFP.
- Cholinergic neurons of airway ganglia contain GFP but most cholinergic projections to airway smooth muscle lack GFP.
- Lack of GFP in cholinergic soma and nerves might reflect unique gene transcription and/or inefficient axonal transport of GFP.

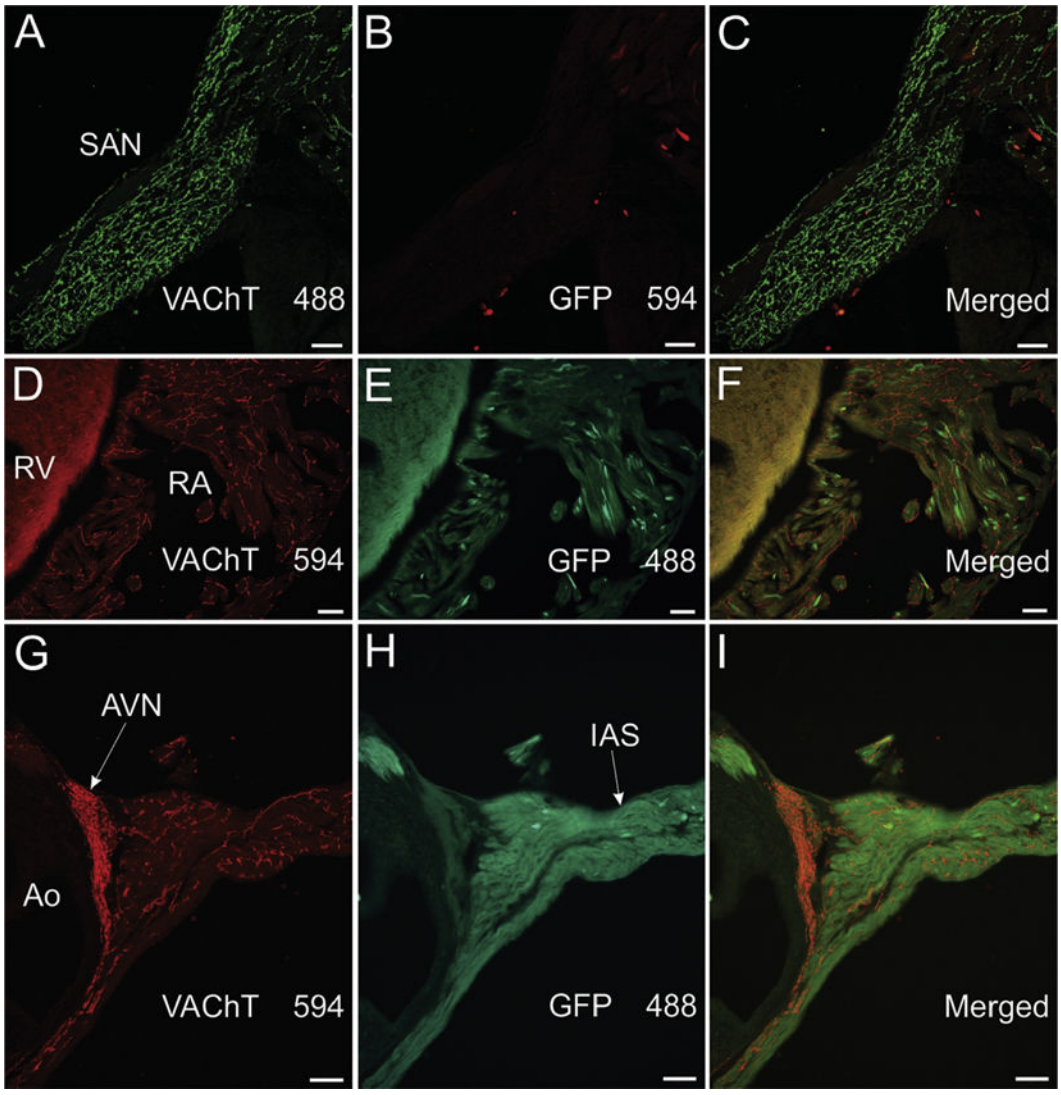

Fig. 1.

VAChT-positive nerves fibers in nodal and contractile regions of atrium lack GFP staining in ChAT^{BAC}-eGFP mice. (A–C) Confocal images of section through the sinoatrial node that was double labeled for VAChT (A) and GFP (B). The rich cholinergic innervation revealed by VAChT staining (A) lacked GFP (B and merged image in C). Alexa Fluor 594 was used to detect GFP in this and some other experiments to assure that lack of staining for GFP could not be attributed to the fluorophore used for detection. (D–I) Standard fluorescence photomicrographs of right atrial and ventricular myocardium (D-F) and the atrioventricular node (AVN) and interatrial septum (IAS)(G-I). Fluorophores used for detection are included with images. Cholinergic innervation of all these regions was stained for VAChT and lacked GFP staining. Ao, aorta; RA, right atrium; and RV, right ventricle. Note that cholinergic nerves are more abundant in atrial regions (A, D, and G) than in RV (D). Scale bars are 50 μm (A–C) and 100 μm (D–I).

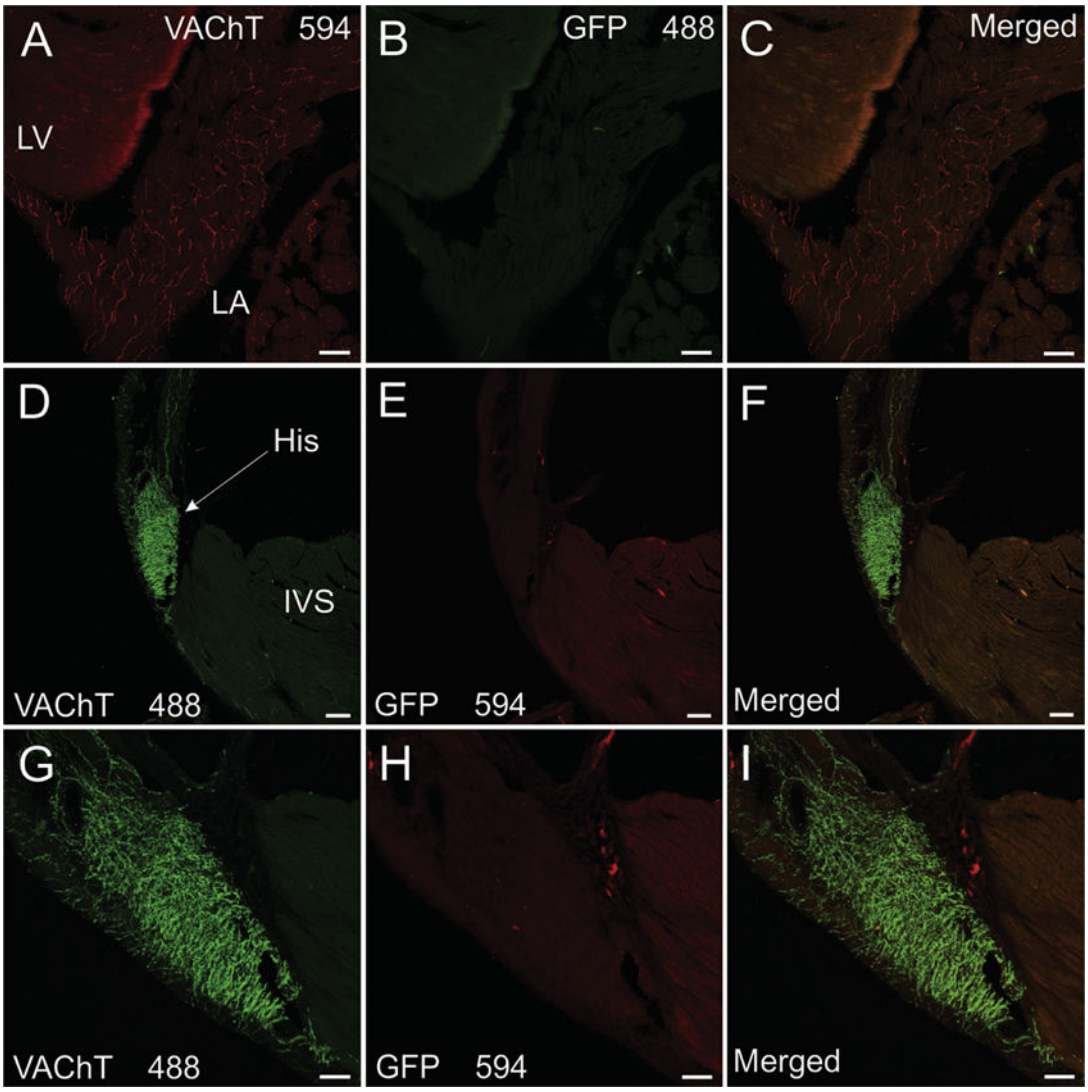

Fig. 2.

VAChT-positive nerves fibers in the left atrium, ventricular conducting system, and interventricular septum lack GFP staining in ChAT^{BAC}-eGFP mice. Fluorophores conjugated to secondary antibodies are specified in relevant panels. (A-C) Confocal projection images showing VAChT-positive cholinergic nerve fibers (A) in the left atrium (LA) and adjacent left ventricle (LV) lack staining for GFP (B and merged image in C). (D–F) Confocal projection images showing VAChT-positive cholinergic nerve fibers (A) in the bundle of His (His) and interventricular septum (IVS) lack staining for GFP (E and merged image in F). (G–I) Higher magnification confocal images of VAChT (G) and GFP (H and merged image in I) in the bundle of His. Scale bars are 100 μm (A-F) and 50 μm (G–I).

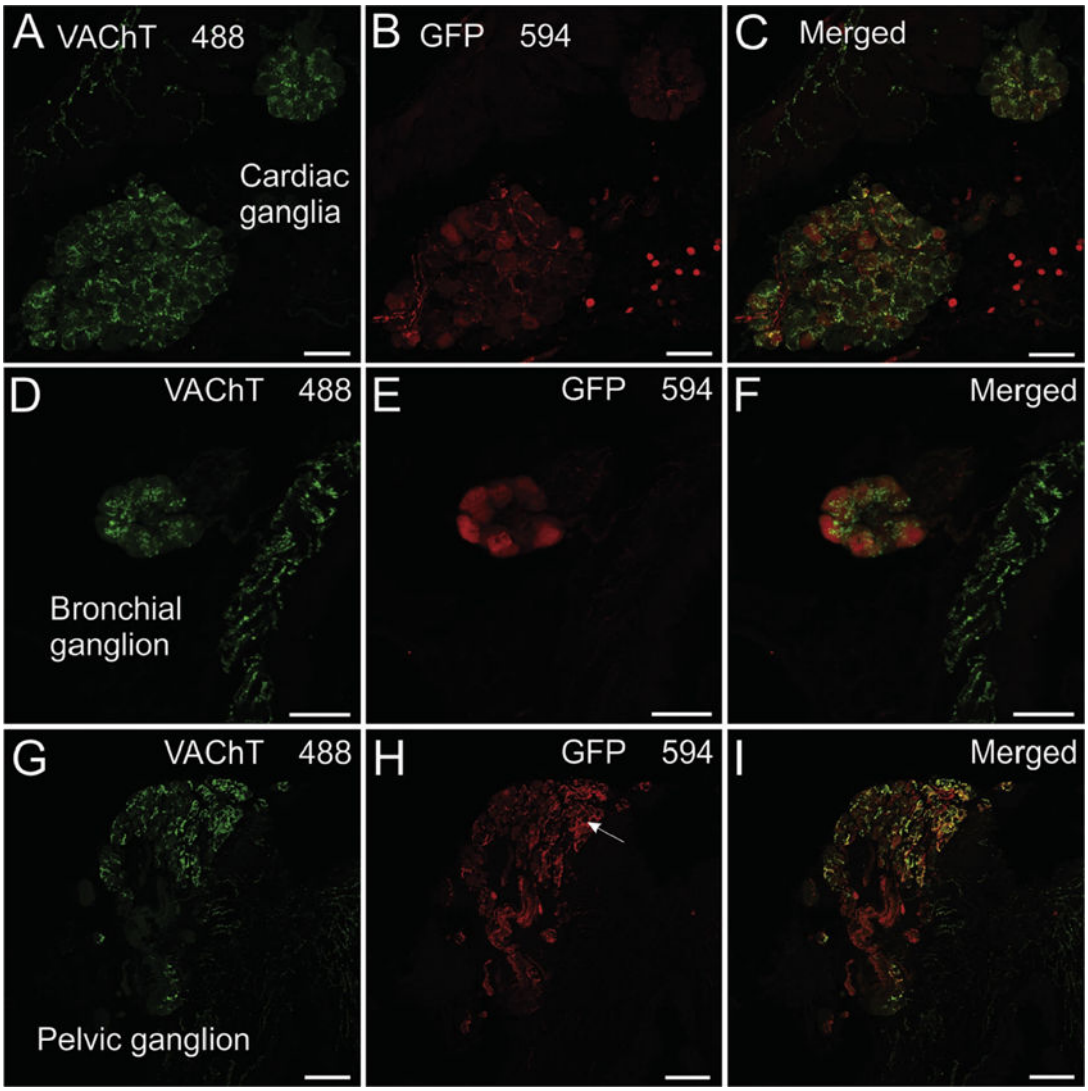

Fig. 3.

Cardiac, airway, and pelvic ganglia exhibit different patterns of GFP localization in ChAT^{BAC}-eGFP mice. An Alex Fluor 594-conjugated secondary antibody was used for detection of GFP. Identical results were obtained with Alexa Fluor 488-conjugated secondary. (A–C) Confocal images showing intrinsic cardiac ganglia labeled for VAChT (A), GFP (B), and a merged image (C). Staining for VAChT was light in neuronal cell bodies and intense in perineuronal varicosities and cholinergic nerves in the adjacent atria (panel A, atria in upper left). Staining for GFP was light to moderate in a few cardiac neurons and in some intraganglionic axons, occasionally seen emanating from neurons in the ganglion. Atrial nerve fibers lacked GFP as did most perineuronal varicosities (B and merged image in C). (D–F) Confocal images showing bronchial ganglion and smooth muscle labeled for VAChT (D), GFP (E), and a merged view (F). Staining for VAChT is light in neuronal perikarya and intense in perineuronal varicosities and cholinergic nerves supplying bronchial smooth muscle (panel D, smooth muscle at right). Staining for GFP was moderate intensity in neuronal perikarya and absent in perineuronal varicosities and

cholinergic nerves in bronchial smooth muscle (E). The merged image (F) shows no colocalization of VAChT and GFP in varicosities or nerve fibers. (G–I) Confocal images showing a pelvic ganglion labeled for VAChT (G), GFP (H), and a merged view (I). Staining for VAChT was light or absent in neuronal perikarya and strong in perineuronal varicosities (G). A similar pattern occurred for GFP with stronger labeling of perikarya (H). The merged image shows extensive colocalization of VAChT and eGFP, especially in perineuronal varicosities (I). Scale bars are 50 μm (A–F) and 100 μm (G–I).

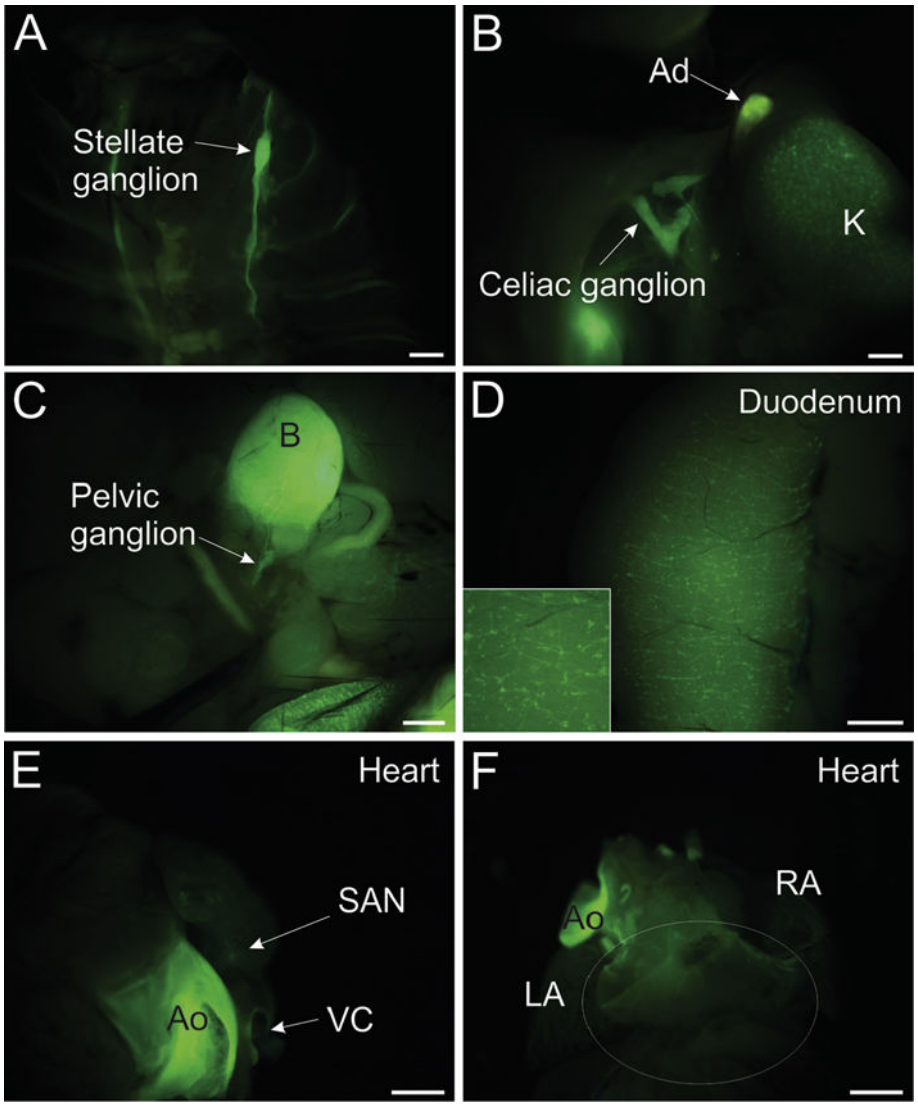

Fig. 4.

Photomicrographs showing that native GFP fluorescence can be detected in several whole tissues of ChAT^{BAC}-eGFP mice but not in the atrial ganglionated nerve plexus on the dorsal atrium. Images were acquired using a stereomicroscope equipped with a Nightsea fluorescence adaptor, as described in Methods. (A) Sympathetic chain ganglia, including the stellate ganglion (arrow) exhibit GFP fluorescence *in situ*. (B) GFP fluorescence associated with preganglionic cholinergic nerves in the celiac ganglion and adrenal gland (Ad) and non-neuronal cholinergic cells in the kidney (K). (C) Major pelvic ganglion and nerves associated with bladder show GFP fluorescence. (D) Enteric nervous system of the duodenum exhibits GFP fluorescence when observed from the serosal surface. Insert shows detail at higher magnification. (E and F) Cardiac cholinergic nerves do not shown GFP fluorescence when viewed under the same conditions as other tissues. Dense innervation of the sinoatrial node (SAN) not apparent in anterior view. Atrial ganglionated nerve plexus associated with dorsal atrium lacks GFP fluorescence. Region of the plexus is indicated by

white oval. Aorta (Ao) exhibits autofluorescence. LA, left atrium; RA, right atrium; and VC, vena cava. Scale bars are 1 mm.

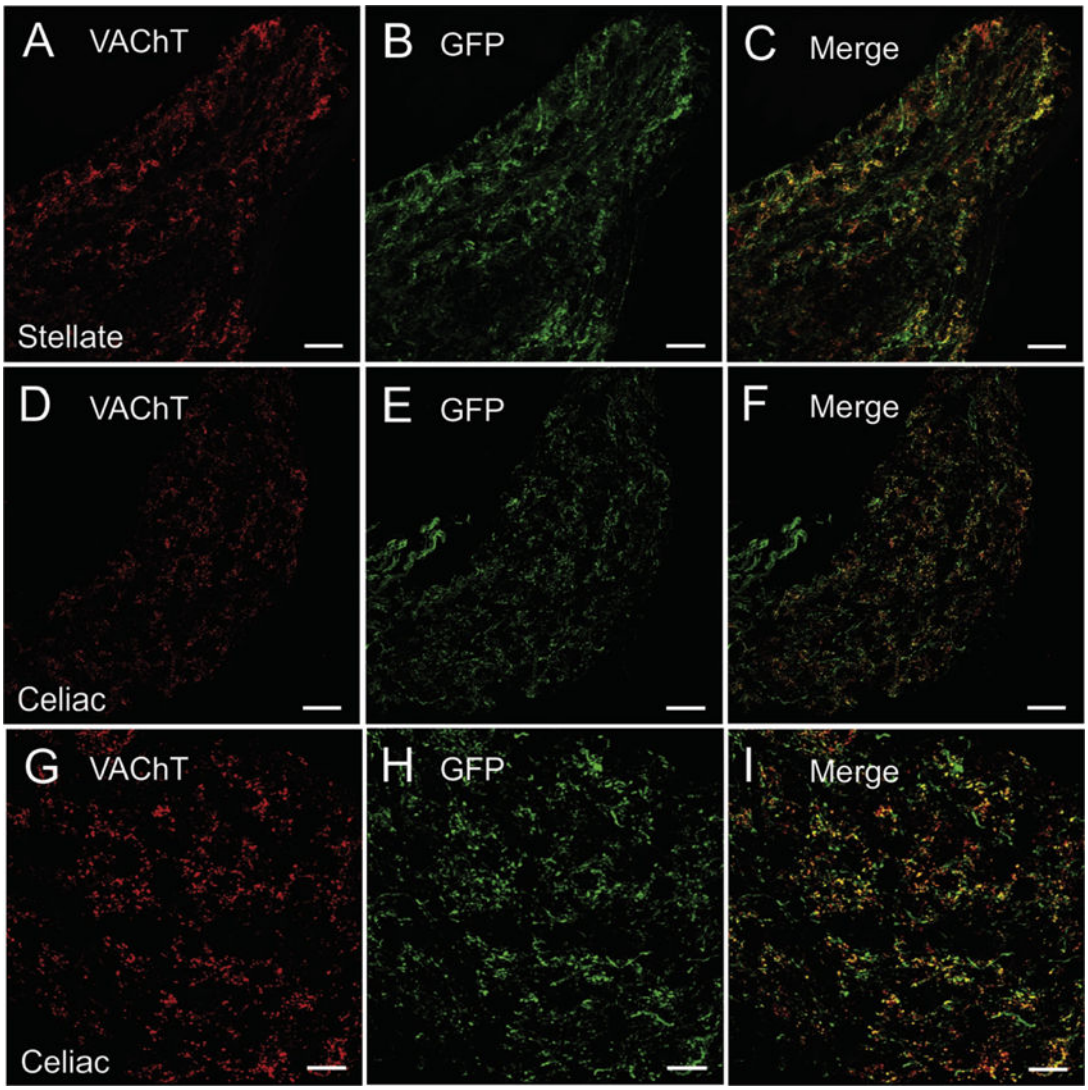

Fig. 5.

VAChT and GFP are localized to cholinergic innervation of sympathetic ganglia. (A-C) Confocal images showing the localization of VAChT (A) and GFP (B) in the stellate ganglion and their colocalization in the merged view (C). (D–F) Confocal images showing the localization of VAChT (D) and GFP (E) in the celiac ganglion and their colocalization in the merged view (F). (G–I) Confocal images showing VAChT (G), GFP (H), and their colocalization (I) in celiac ganglion at a higher magnification. For this experiment VAChT was detected using Alexa Fluor 594 and eGFP with Alexa Fluor 488. Scale bars are 50 μm (A–F) and 25 μm (G–I).

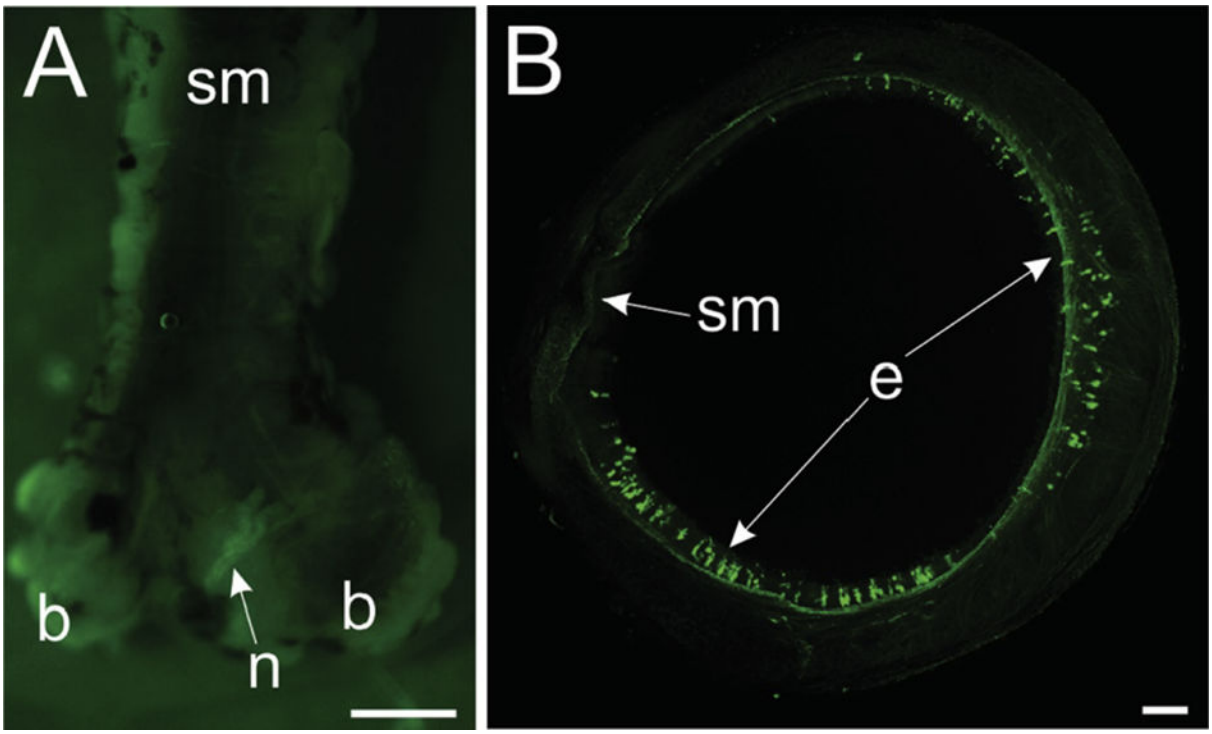

Fig 6.

Photomicrographs showing that native GFP fluorescence can be detected in trachea epithelial cells but not in tracheal smooth muscle. (A) Fluorescence image of whole trachea dissected from ChAT^{BAC}-eGFP mouse with smooth muscle (sm) region facing up. Image was acquired using a stereomicroscope equipped with a Nightsea fluorescence adaptor, as described in Methods. Exposure time was increased to over 1 sec to visualize the trachea. A nerve (n) at the bifurcation of the trachea was the only structure showing GFP fluorescence. (B) Confocal image of unfixed tracheal ring shows prominent native GFP fluorescence of scattered epithelial cells (e) but no GFP fluorescence associated with cholinergic nerves in tracheal smooth muscle. This maximum projection image was generated from 88 optical sections spanning 210 μm in the z-axis. Scale bars are 1 mm (A) and 100 μm (B).

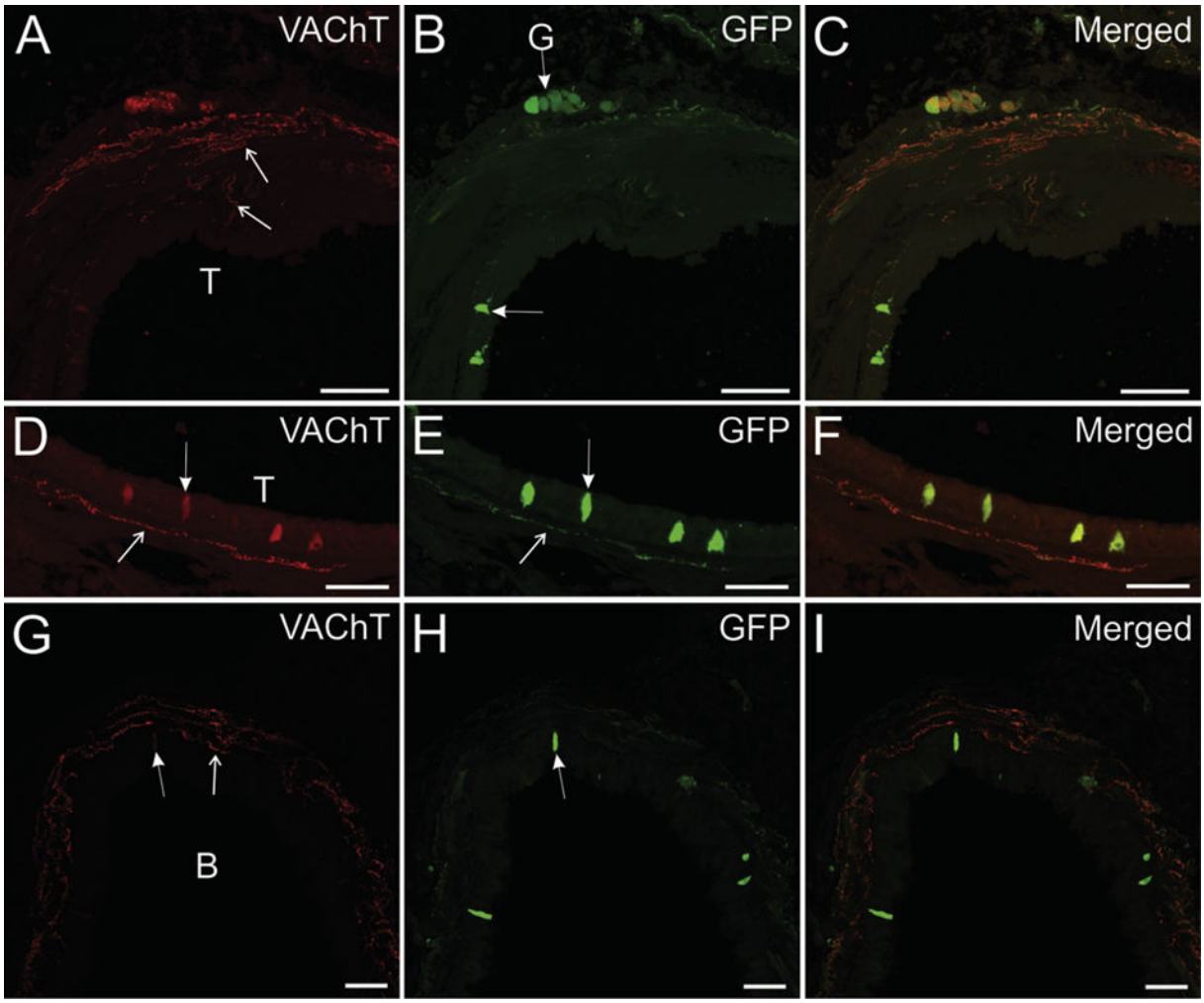

Fig. 7.

Confocal images of trachea and bronchus showing VAChT dominance in innervation of airway smooth muscle and a ganglion and GFP dominance in ganglionic neurons and epithelial cells. (A–C) Nerve fibers in tracheal smooth muscle and tracheal ganglion stain intensely for VAChT (A). A few VAChT+ nerve fibers stain lightly for GFP, and tracheal neurons and epithelial cells stain intensely for GFP (B and C). (D–F) Some GFP+ cholinergic epithelial cells (E and F) exhibit light to moderate staining for VAChT (D). A subepithelial nerve fiber stains intensely for VAChT (D) and lighter for GFP (E). (G–I) Cholinergic nerve fibers supplying bronchial smooth muscle stain intensely for VAChT (G), and a few nerve fibers exhibit light staining for GFP (H). Bronchial epithelial cells stain intensely for GFP (H and I). Left arrow in G indicated light staining for VAChT in one epithelial cell. Arrows with line tip indicate nerve fibers. Arrows with solid tip indicate epithelial cells. T, trachea and B, bronchus. Scale bars are 100 μm (A–C) and 50 μm (D–I).

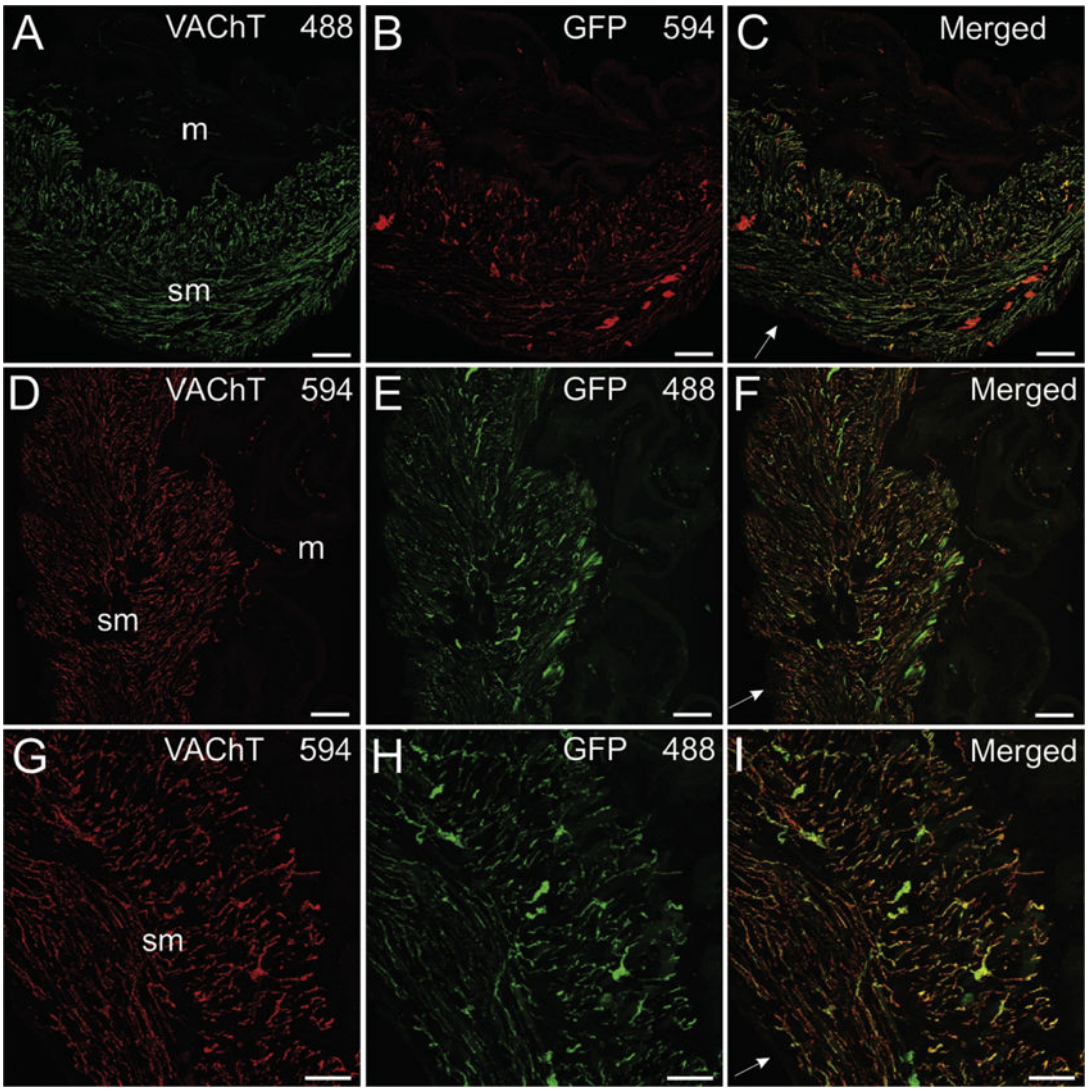

Fig. 8.

VAChT and GFP are localized to cholinergic innervation of bladder. VAChT and GFP were detected with Alexa Fluor 488 and 594, respectively, in panels A–C. Fluorophores were switched for sections in panels D-I. VAChT-positive nerve fibers are very dense in the smooth muscle (sm) layers of the bladder wall (A, D, and G) and relatively sparse in the muscosal (m) regions (A and D). Labeling for eGFP shows a similar pattern to that for VAChT (B, E, and H), and there is extensive colocalization of these markers (C, F, and I). The intensity of labeling for eGFP was less than that for VAChT in many nerve fibers, regardless of the fluorophore combination used. Scale bars are 100 μm (A–F) and 50 μm (G–I).

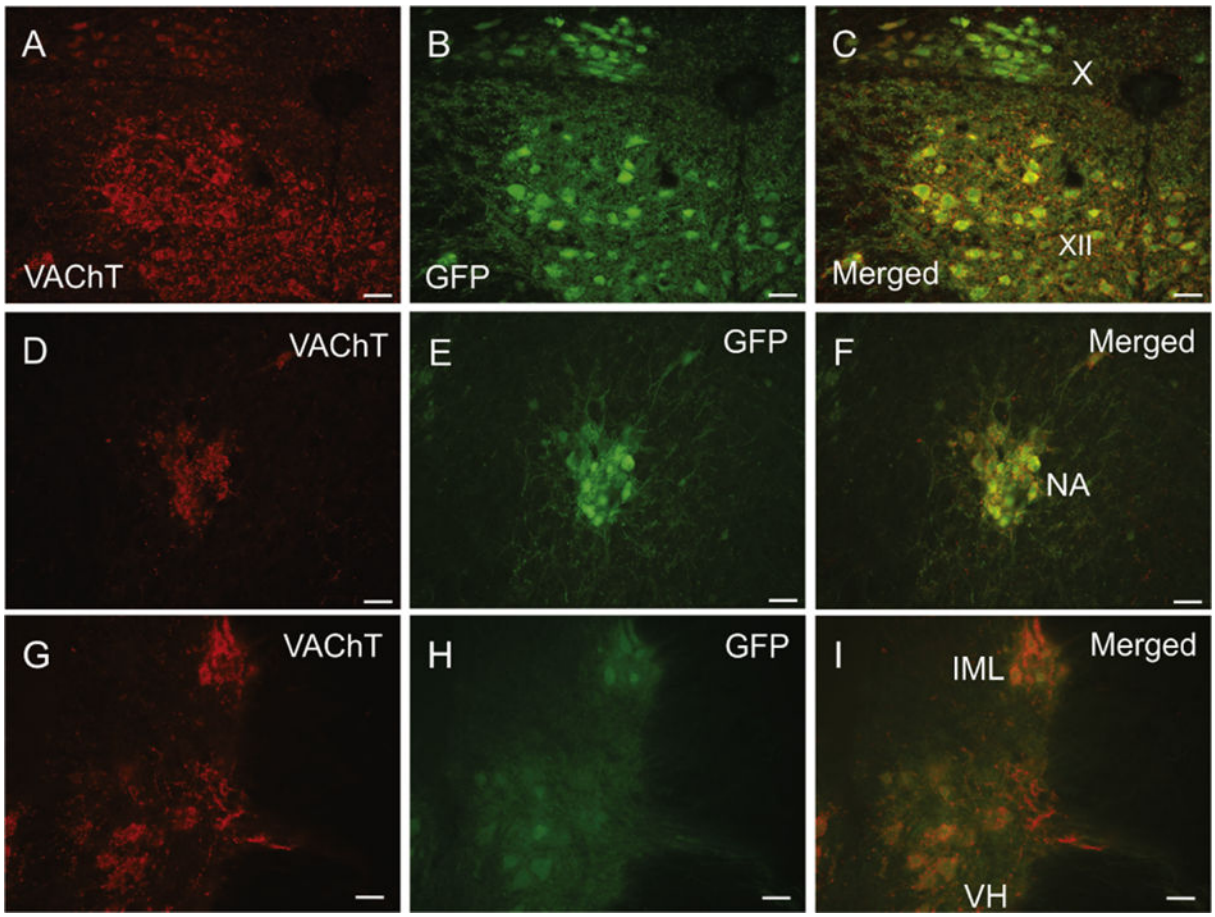

Fig. 9.

Photomicrographs showing the colocalization of VAChT and GFP in cholinergic efferent neurons of the medulla and spinal cord. (A–C) View of dorsal motor nucleus of the vagus (X) and hypoglossal nucleus (XII) showing VAChT (A), GFP (B) and a merged image (C). (D–F) Nucleus ambiguus (NA) double stained for VAChT (D), GFP (E) and merged image (F). (G–I) Intermediolateral (IML) nucleus of L1 spinal cord and motor neurons in ventral horn stained for VAChT (G), GFP (H) and merged image (I). Scale bars are 50 μm.

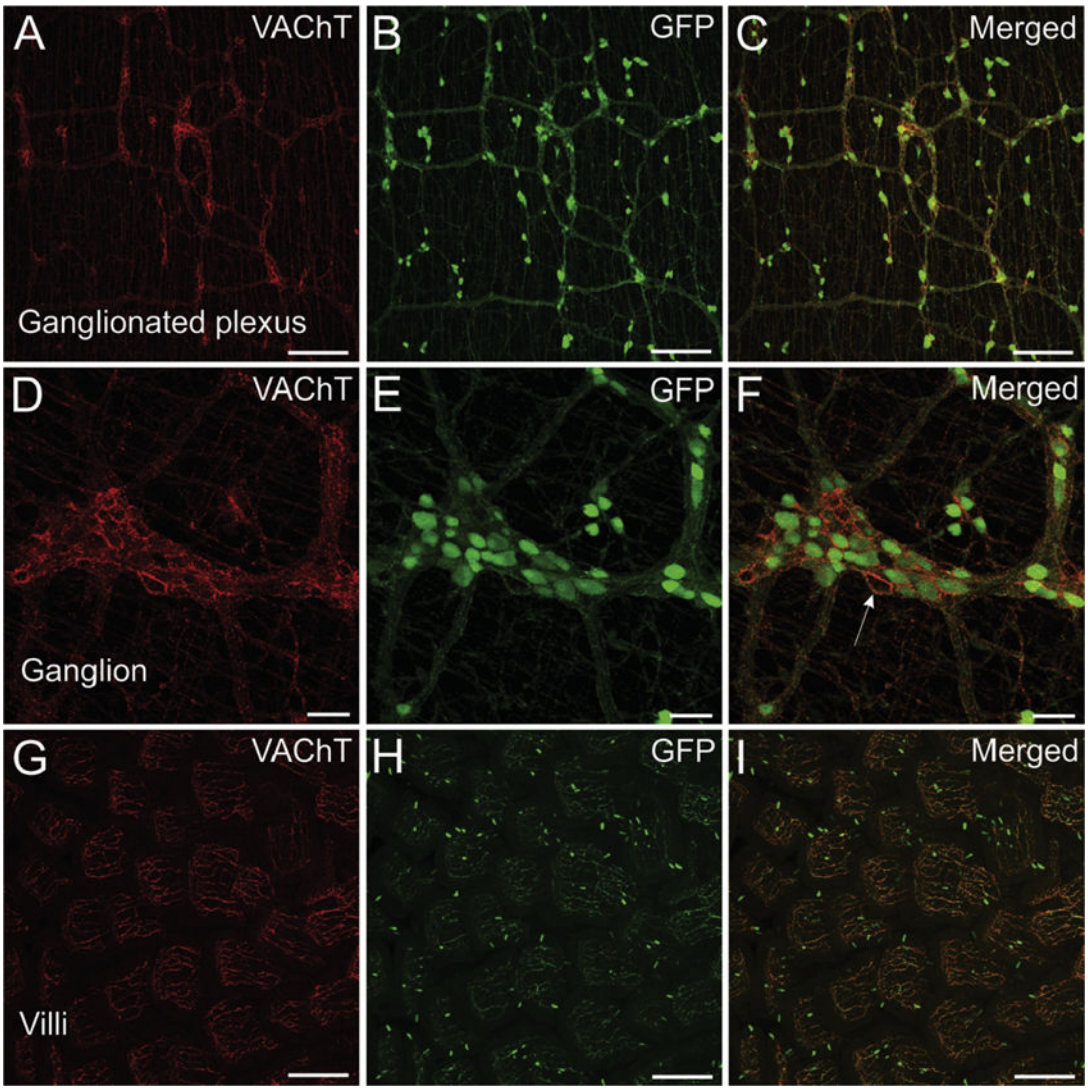

Fig. 10.

Confocal images showing localization of GFP and VAChT in a whole mount of duodenum. (A–C) VAChT is localized to nerve fibers in the ganglionated nerve plexus (A). GFP is also localized to the nerve plexus, but unlike VAChT, GFP is also abundant in neuronal perikarya located in ganglia and along the plexus (B). (D–F) Higher magnification view of a ganglion. Nerve fibers in the plexus and surrounding neurons stain intensely for VAChT (D). Staining for GFP is intense in perikarya but relatively light and sparse in perineuronal varicosities compared to labeling for VAChT (E and F). Arrow indicates non-cholinergic neuron surrounded by varicosities that stain intensely for VAChT and much lighter for GFP. (G–I) Nerve fibers in the intestinal villi stain intensely for VAChT and GFP, but scattered epithelial cells only stain for GFP. A–C show maximum projection images generated from 23 optical sections spanning 53 μm in the z-axis. D–F show maximum projection images generated from 16 optical sections spanning 36 μm in the z-axis. G–I show maximum projection

images generated from 64 optical sections spanning 152 μm in the z-axis. Scale bars are 200 μm (A–C and G–I) and 50 μm (D–F).

Table 1

Qualitative summary of VAChT and GFP presence in major elements of the autonomic nervous system and enteric nervous system of ChAT^{BAC}-eGFP mice.

Region/cellular location	VAChT	GFP
Autonomic preganglionic neurons		
Dorsal motor nucleus	+	+++
Nucleus ambiguus	+	+++
Intermediolateral cell column	+	+++
Autonomic ganglia		
Sympathetic ganglia		
Stellate ganglion		
Perikarya	–	–
Nerve fibers/varicosities	+++	+++
Celiac ganglion		
Perikarya	–	–
Nerve fibers/varicosities	+++	+++
Parasympathetic ganglia		
Intrinsic cardiac ganglia		
Perikarya	+	±
Nerve fibers/varicosities	+++	±
Airway ganglia		
Perikarya	+	++
Nerve fibers/varicosities	+++	–
Pelvic ganglia		
Perikarya		
Cholinergic	+	++
Non-Cholinergic	–	–
Nerve fibers/varicosities	+++	+++
Parasympathetic target tissues		
Heart		
Sinoatrial node	+++	–
Atrial myocardium	+ to ++	–
Atrioventricular node	++++	–
Bundle of His	++++	–
Ventricular myocardium	±	–
Airway smooth muscle	+++	±
Bladder		
Smooth muscle	+++	++
Mucosa	+	+
Enteric nervous system		
Ganglia		
Perikarya	–	+++

Region/cellular location	VAChT	GFP
Varicosities	+++	±
Ganglionated nerve plexus	+++	+++

Grading scale: –, labeled nerve fibers or perikarya not detected; ±, low abundance and/or staining intensity, + through ++++, increasing abundance of labeled nerve fibers or intensity of staining in perikarya.